CHEMISTRY OF MATERIALS

Article

pubs.acs.org/cm

Supramolecular Diversity through Click Chemistry: Switching from Nanomicelles to 1D-Nanotubes and Tridimensional Hydrogels

Mohyeddin Assali,[†] Juan-José Cid,[†] Inmaculada Fernández,[‡] and Noureddine Khiar[†,*]

[†]Asymmetric Synthesis and Functional Nanosystems Group, Instituto de Investigaciones Químicas (IIQ), CSIC and Universidad de Sevilla, C/Américo Vepucio 49, 41092 Seville, Spain

[‡]Departamento de Química Orgánica y Farmacéutica, Universidad de Sevilla, C/García González 2, 41012 Seville, Spain

Supporting Information

ABSTRACT: The size and shape of nanoparticles are of prominent importance for their biological activities and for their application as smart drug delivery systems. Thus, synthetic designs allowing divergent synthesis of nanoscale materials with controlled size, morphology, and surface chemistry are currently highly desirable, but they remain a major challenge. Herein, we report a simple method for the creation of supramolecular diversity from structurally related diacetylenic-based glycolipids. We have found that neoglycolipids with an amide function between the hydrophilic and hydrophobic part of the amphiphile afford tridimensional micelles, while those having a triazole self-organize into 1D-nanotubes. Additionally, at higher concentrations, the clicked amphiphiles form hydrogels through three-dimensional networks of bundled nanotubes. Photopolymerization of the obtained nanomaterials leads to the formation of conjugated polydiacetylene backbone of alternating enyne groups, which rigidify glyconanomaterial structures enhancing their physical stability. The obtained nanostructures were extensively characterized using transmission electron microscopy (TEM), scanning electron microscopy (SEM), and atomic force microscopy (AFM) techniques, enabling the confirmation of the formation of tubular structures in water for all triazolo-substituted neoglycolipids and micellar structures for the glycolipid containing an amide group. This fact refutes the so-called isosteric character of 1,2,3-triazole and amide groups, at least, at the supramolecular level and point out to the possibility of using the CuAAC between azides and alkynes to create supramolecular diversity at the nanoscale. The functionality of the gel was, moreover, evaluated as a nanocontainer for the incarceration and controlled release of the antitumoral topotecan.

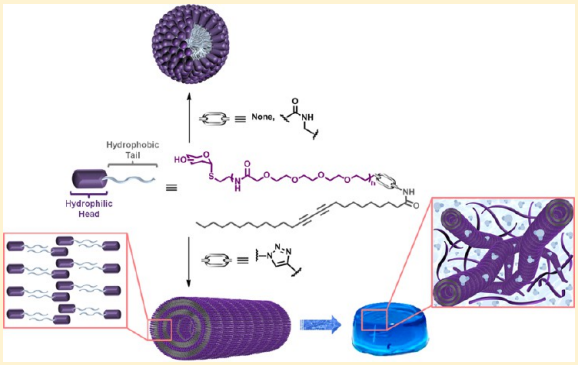

KEYWORDS: *click chemistry, supramolecular self-assembly, carbohydrate-coated robust nanomaterials, PDA-based hydrogels, PDA-based micelles, PDA-based lipid nanotubes*

INTRODUCTION

The advent of nanotechnology has increased the need for bottom-up approaches that can generate complex nanoscale systems from simple molecules or architectures.[1−6] In this sense, chemical self-assembly, the spontaneous association of molecules into well-defined structures held together by noncovalent interactions, is one of the most attractive approaches for constructing complex supramolecular nanostructures.[7−10] Hierarchical processes typical of chemical self-assembly, spontaneously produce ordered multivalent systems,[11−14] valuable tools in biology and nanotechnology, starting from prefunctionalized monomers.[15−20] As a result of the deep impact of nanoscale materials in the nascent field of nanomedicine, self-assembled nanostructures taking place in water are receiving special interest, as they can be directly applied in important biological processes.[21−24] Structure−activity relationship studies have shown that, beside the surface chemistry, the topology and size of nanoscale molecules are key factors for their biological activities, including their cellular uptake, circulation time, interaction with specific receptors, and their application as smart drug delivery systems.[25−27] In this sense, while spherical nanomaterials, preferentially with 50 nm size, are well suited for processes proceeding through a rapid cellular uptake, 1D-rodlike structure are more appropriate for those requiring improved circulation time. On the other hand, it has recently been reported that whereas spherical mannose-coated micelles are potent inhibitors of a globular lectin, concanavalin A, the mannose-coated 1D-cylindrical micelles are more suited for the inhibition of bacterial motility.[28,29] Thus, synthetic designs allowing the divergent synthesis of functionalized nanoscale materials with varied morphologies preferentially from a common intermediate, with no additional synthetic cost are highly desirable. Yet, designing molecular materials in which the self-assembled nanostructures are predetermined by molecular architecture remains a major challenge, especially if self-assembly is used to control the size, the morphology, and

Received: July 8, 2013
Revised: September 30, 2013
Published: October 2, 2013

dx.doi.org/10.1021/cm4022613 | *Chem. Mater.* 2013, 25, 4250−4261

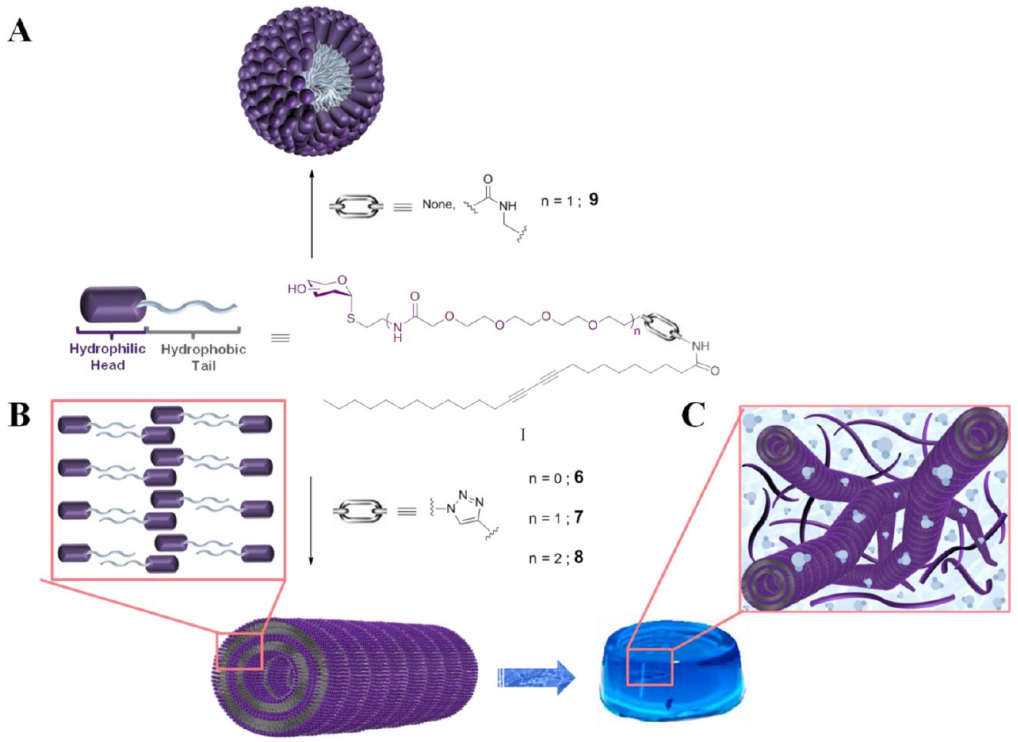

Figure 1. Supramolecular self-organization of sugar-coated PDA-amphiphiles, showing the crucial role of the ligation group used to link the diacetylenic hydrophobic and hydrophilic parts: Starting from a common intermediate a simple change of the amide function to a triazole group in **I** allows the formation of 1D-nanotubes (B) which evolve to tridimensional gels (C) instead of forming tridimensional micelles (A).

the surface chemistry of the final nano-objects.[30] For example, a large variety of low molecular mass organogelators (LMOGs) have been reported to form gels through three-dimensional networks of bundled nanofibers and nanoribons.[31−35] The development of this nanoengineering field is exemplified by recent applications of molecular gels in the fields of tissue engineering,[36−38] biomineralization,[39,40] molecular electronics,[41,42] and drug delivery.[43−46] However, the lack of knowledge of the fundamental parameters behind self-assembly into gels difficults the design of systems in which molecular modification would control nanoscale assembly that ultimately endows specific materials function.[47] A special concern about the nanoscale materials formed by chemical self-organization, and which limits their practical applications, is their limited stability. The utilization of micelles for instance in biomedical processes is limited by its sensitivity to dilution,[48] while hydrogels are easily collapsed or changed by small perturbations in the environmental conditions.[49] Therefore, there is great interest in the synthesis of monomers that can be further manipulated in the supramolecular state in order to endow the nanoassemblies with physicochemical stability. Diacetylenic amphiphiles are well suited for such a proposal, as they can undergo topochemical reactions upon UV-irradiation or thermal stimuli, leading to the anisotropic formation of poly(diacetylene) (PDA) in the crystalline state.[50,51] Closely packed and properly ordered diacetylenes amphiphiles undergo a smooth and clean photopolymerization via 1,4-addition reaction, affording functional PDA-nanomaterials with enhanced stability and interesting chromatic properties.[52−56] Indeed, PDAs exhibit an intense blue color due to the absorption of the enyne cross-linked framework in the visible region. Furthermore, phase transitions of the conjugated backbone of the polymer can be induced, resulting in modification of the delocalized conjugated electronic networks, thereby resulting in dramatic blue-to-red transformations. The structural/colorimetric transformations of PDA assemblies can take place in response to heat (thermochromism),[57−59] organic solvents (solvatochromism),[60,61] mechanical stress (mechanochromism),[62,63] magnetic fields (magnetochromism),[64] and ligand−receptor interactions (affinochromism or biochromism).[65−69] These exceptional physicochemical properties have boosted the utilization of diacetylenic amphiphiles as self-organizing monomers for the synthesis of various nanostructured materials, including liposomes,[70] micelles,[71] films,[72] and nanotubes,[73] mainly for sensing proposals.

Based on these premises, in the present work, we report a new design allowing the divergent synthesis of PDA-based nanomaterials with different morphologies. We have found that, in the case of amphiphilic neoglycolipid I (Figure 1, center), the ligation group used to link the diacetylenic hydrophobic part and the hydrophilic part formed by an oligoethyleneoxide-tethered sugar play a crucial role in their self-organization. While diacetylenic-based glycolipids with an amide function between the hydrophilic and hydrophobic part afford micellar structures (Figure 1A), those with an additional triazole ring—obtained by click ligation of relatively similar partners—afforded 1D-tubular microstructures (Figure 1B). Hierarchical aggregation and entanglement of the nanotubes in water allow us to develop novel hydrogels (Figure 1C), implementing the attractive functions of the hollow cylinders. Subsequent photopolymerization turns out stable and blue colored nanomaterials responsive to external stimuli such as heat and solvents. The structure, aggregation and self-assembly of the formed nanomaterials have been investigated by nuclear magnetic resonance (NMR), infrared spectroscopy (IR), transmission electron microscopy (TEM), scanning electron

dx.doi.org/10.1021/cm4022613 | *Chem. Mater.* 2013, 25, 4250−4261

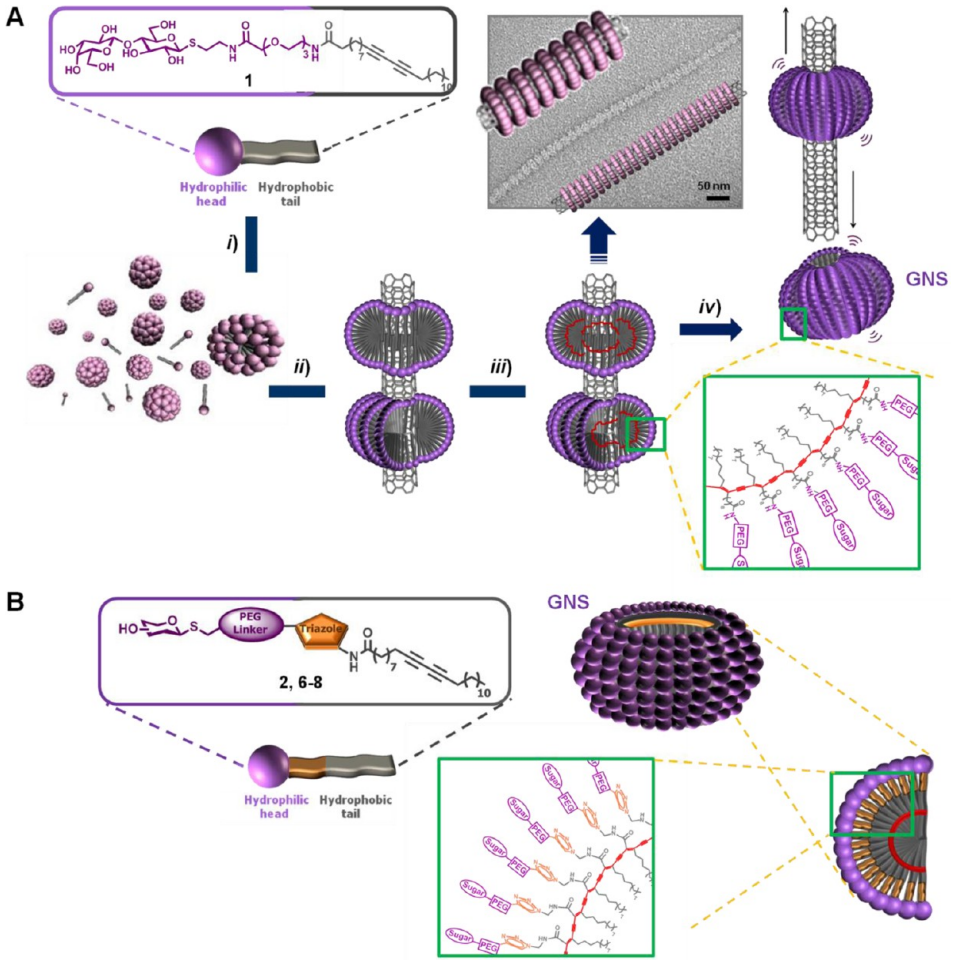

Figure 2. Procedure for SWCNT/**1** nanoassembly formation and synthesis of glyconanosomes (GNS). (A) (i) Formation of micelles by mixing neoglycolipid **1** above its critical micelle concentration (CMC) in water. (ii) Sonication-promoted supramolecular self-assembly of neoglycolipid **1** in concentric hemimicelles around SWCNTs. (iii) Intermolecular photopolymerization of neoglycolipid **1** hemimicelles into homogeneous glyconanorings (GNRs). Above, TEM micrograph of SWCNT/**1** nanoassemblies and their idealized representative figures. (B) Structural and chemical composition of a sought glyconanosome in the present work.

microscopy (SEM), and atomic force microscopy (AFM). One of the resulting gels was then assayed as a nanocontainer for the inclusion and release of cytotoxic topotecan drug as a first step toward their use as smart drug delivery system. As far as we know, this is the first example of supramolecular nanotube hydrogel, based on amphiphilic diacetylene building blocks,[74] although some bolaamphiphilic diacetylenes are known to gel organic solvents or a mixture of water and polar organic solvents.[75−78]

RESULTS AND DISCUSSION

Synthesis of "Clicked" Diacetylene-Based Glycolipid Monomers. We have recently reported a bottom-up approach for the water-solubilization and biofuncionalization of CNTs (Figure 2)[79,80] based on the self-organization of amphiphilic molecules on the CNTs sidewalls.[81−84] In the case of neoglycolipid **1**, the design include a tetraethyleneglycol-tethered lactose moiety responsible of the water solubilization. Opposite to the external exposition of the functional glycoligand, a 25 carbon-based hydrophobic tail was included for efficient van der Waals interactions with the CNT sidewalls, bearing furthermore, a photopolymerizable diacetylenic function (Figure 2A).

Preliminary mechanistic studies have shown that neoglycolipid **1** first self-organizes into micelles in aqueous solution, then undergoing a hemimicellar arrangement on the solid surface of the CNTs. Indeed, a TEM analysis of a water solution containing **1** over the critical micellar concentration (CMC) shows the formation of spherical micelles with 12 nm diameter (Figure 2A, step i). The micellar solution of neoglycolipid **1** was capable of facilitating and promoting the deaggregation of SWCNTs bundles, giving rise to stable dispersions of assembled SWCNTs/**1** nanoconstructs. Interestingly, TEM, SEM, and AFM analyses showed that compound **1** self-assembled on the SWCNTs surfaces in a supramolecular fashion, resulting in rings made of rolled-up half cylinders (Figure 2A, step ii). The photopolymerization of the diacetylene function upon ultraviolet irradiation (254 nm) afforded a conjugated polydiacetylene backbone of alternating enyne groups (Figure 2A, step iii), which rigidified the inner core of each hemimicelle, resulting in robust polymerized glyconanorings (GNRs) around the nanotube in an abacus-like geometry. Subsequently, ultrasonication of the nanoconstructs allowed the slid of neutral glyconanorings out of their assemblies with SWCNTs. These new disc-shaped nanomaterials, called glyconanosomes (GNSs), with a 35−55 nm length diameter have a hydrophobic inner core surrounded by a

dx.doi.org/10.1021/cm4022613 | *Chem. Mater.* 2013, 25, 4250−4261

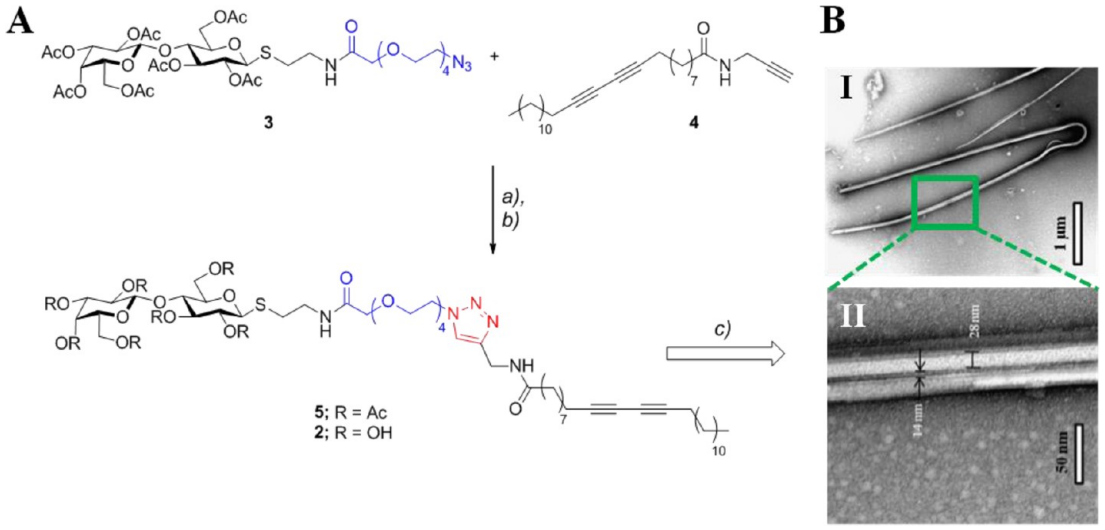

Figure 3. (A) Convergent synthesis of neoglycolipid **2** by CuCAAC: (a) CuI, DIPEA, CH_2Cl_2, rt, overnight; (88%). (b) (i) NaOMe, MeOH, rt; 1 h. (ii) Amberlyst Ir-120; (67%). (c) (i) H_2O, 70 °C, (ii) *hv* (254 nm), 24 h. (B) A large-scale height (I) and enlarge phase (II) TEM images of spherical nanotubes formed by self-organization of neoglycolipid **2** in water.

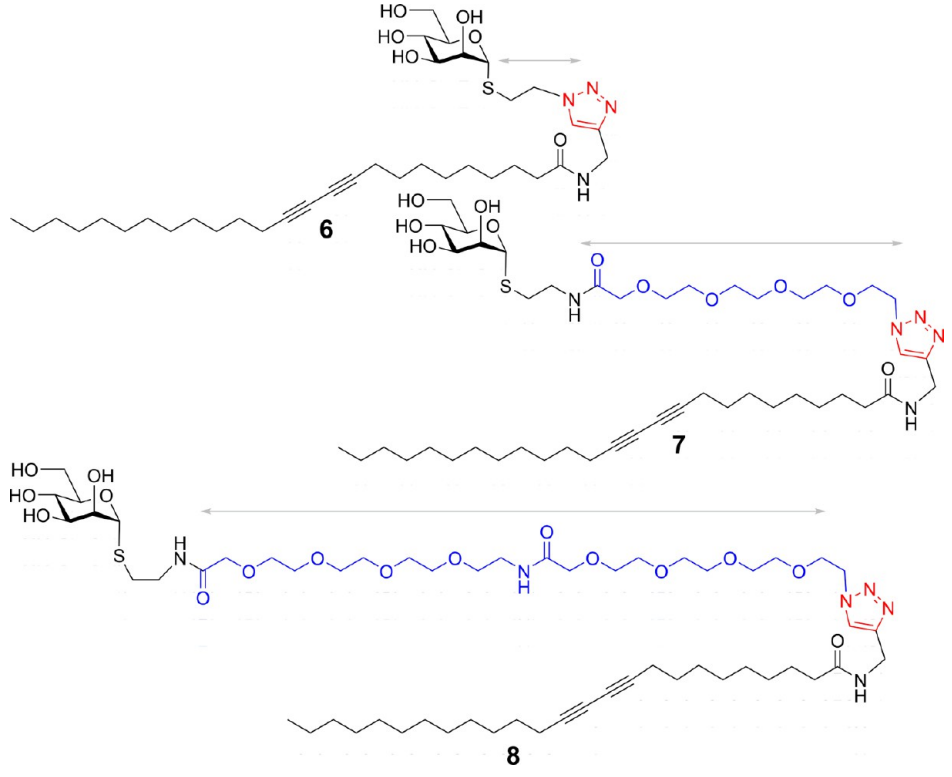

Figure 4. Chemical structures of neoglycolipids **6**–**8** with increasing length of the spacer in between the diacetylenic tail and the sugar headgroup.

hydrophilic tetraethyleneglycol chain capped by a biodetectable lactose moiety are well-suited candidates for active drug delivery.[85] In order to fine-tune the hydrophobicity and functionality of the inner core of the GNSs, we thought in including an aromatic ring able to establish further interactions with guest molecules through $\pi-\pi$ interactions (Figure 2B). As an aromatic fragment, we choose to introduce a triazole ring connecting the hydrophilic and hydrophobic parts of the amphiphile by using the unrivalled copper(I)-catalyzed azide–alkyne cycloaddition (CuAAC), the paradigmatic example of "click chemistry".[86−88] The synthesis of the required diacetylenic lipid **2** (Figure 3A), functionalized with thiolactose has been performed in a convergent manner using a similar approach than that for compound **1**. The click reaction of the advanced azido intermediate **3** used in the synthesis of **1** and *N*-(2-propynyl)pentacosa-10,12-diynamide **4** using Cu(I) in the presence of Hunig base in methylene chloride, afforded regioselectively the 1,2,3−triazole derivative **5** in excellent 88% yield, (Figure 3A, step a). Finally, a Zemplen deacetylation in methanol afforded the desired thiolactose-based neoglycolipid **2,** as depicted in Figure 3A, step ii.

Surprisingly, despite its structural similarity with compound **1**, neoglycolipid **2** was unable to solubilize CNTs in water, consequence of its incapacity to form micelles. Indeed, a study

dx.doi.org/10.1021/cm4022613 | *Chem. Mater.* 2013, 25, 4250−4261

of water solutions of neoglycolipid **2** shows that it self-organizes forming 1D-tubular nanostructure, able to gel water at concentration of 1% w/w. TEM analysis of a negatively stained diluted solution (0.1%) of **2** showed the formation of nanotubes with several micrometer lengths, an outer diameter of 70 nm, an inner diameter of 14 nm, and a membrane thickness of 28 nm (Figure 3A, step iii).

In order to decipher the exact role of the triazole ring on the self-organization of **2** into 1D tubular nanostructure, we designed various related neoglycolipids and studied their self-organizations. To fine-tune the hydrophilic/hydrophobic balance of the designed amphiphiles and generalize the observed effect to other sugar coated nanomaterials, we used as sugar headgroup the monosaccharide mannose, instead of the disaccharide lactose. The neoglycolipids designed are depicted in Figure 4 and include neoglycolipid **6** with no hydrophilic spacer between the hydrophobic moiety and the sugar headgroup, the neoglycolipid with a hydrophilic spacer derived from a tetraethyleneglycol **7**, and, finally, the neoglycolipid **8** with a hydrophilic spacer 2-fold larger than in compound **7**. These triazolo-substituted neoglycolipids were synthesized by means of a convergent synthetic routes similar to that used for the synthesis of **2**, employing as a key reaction the regioselective CuAAC reaction between the corresponding azido-substituted sugars and the trialkyne *N*-(2-propynyl)-pentacosa-10,12-diynamide **4**.

Study of the Self-Association of the "Clicked" Diacetylene-Based Glycolipid Monomers in Water. Once in hand, each neoglycolipid was suspended in Milli-Q water, affording diluted solutions (0.1%) that were subsequently heated beyond the melting temperature of pure solids (up to 50 °C in all cases), so ensuring the complete deaggregation and homogeneity of the mixtures (qualitatively showing as noncloudy solutions). Then, they were slowly cooled to room temperature, observing the apparition of homogeneous white fibrillar suspensions for all the neoglycolipids **6**–**8** studied. Once all the basic supramolecular assemblies were attained, subsequent photopolymerization reactions comprising the diynic fragment into poly(diacetylene) polymer (PDA) derivatives were carried out by irradiation at 254 nm using a UV lamp. A series of covalently fixed PDA-derived structures with a dark-blue color were obtained, accompanied by the appearance of an absorption band in the visible region with a maximum at 605 nm (Figure 5).

PDA-based nanomaterials are responsive to various external stimuli and as such, are excellent sensors able to detect and report the change occurring in their surrounding medium. In this sense, heating the clicked glyconantubes **6** and **7** at 100 °C for 5 min induces a drastic chromatic change from blue to red (Figure 5C, spectra I and II) with the concomitant disappearance of the band at 605 and the appearance of a new band at 505 in the UV–vis spectra. Beside their characteristic thermochromism, glyconanotubes are also sensitive to the solvent present in the medium (solvatochromism) as shown by the change to red of the fibrillar nanostructures upon adding methanol.

Next, the resulting structures and morphologies of the diluted mixtures of clicked nanomaterials were analyzed by TEM and AFM microscopies (Figure 6). In all the series, micrometer length glyconanotubes were formed (Figure 6A) having relatively similar internal diameters (around 15 nm) and external diameters varying from 46 nm for **6**, 54 nm for **7** to 75 nm for **8**, (Figure 6B). These results, demonstrate that the self-

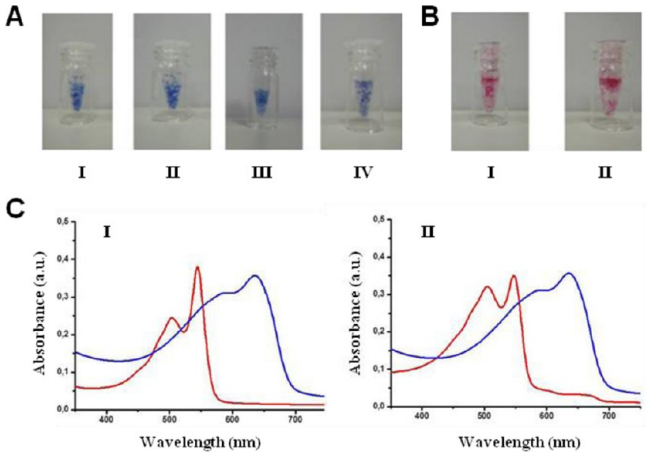

Figure 5. (A) Photographs of vials showing the formation of blue colored PDA-based nanotube suspensions after photopolymerization of neoglycolipids **2** (I), **6** (II), **7** (III), and **8**(IV). (B) Photographs of vials highlighting the thermochromatic changes from blue to red of the nanotube suspensions derived from **6** (I) and **7** (II) upon heating at 100 °C for 5 min, characterized by disappearance of the band at 605 and the appearance of a new band at 505 in the UV–vis spectra (C).

organization of clicked diacetylenic glycolipids is indeed independent of the hydrophobic/hydrophilic balance of the amphiphile and consistently lead to 1D-hollow glyconanotubes with relatively similar structures in form, size, and thickness.

Moreover, AFM (specially the AFM-3D image) of glyconanotube **7** (Figure 6C and D) corroborated the tubular nature of the nanoconstructs, reflecting consecutive striations on the tube surfaces, as a consequence of the regular folding, and curl of rolled tapes composed from the superposition of neoglycolipidic bilayers (see also Figures S7 and S8 in the SI and the tubular model depicted in Figure 8C *vide infra*).

Gelation Study. All the clicked neoglycolipids with the triazole ring led to the formation of gel-state at 1% concentration, and in the following section, we will detail the synthesis, characterization, and use as nanocontainer for the stabilization and controlled delivery of antitumoral drug of the gel formed from neoglycolipid **7**. An aqueous solution of neoglycolipid **7** (1%) was heated at 50 °C for 30 min, affording upon cooling to room temperature a white waxy material whose jelly nature was proved by the method of being "stable to inversion of the container", highlighting a complete absence of flow (Figure 7).[89] The stability of the nonpolymerized gel at room temperature and in absence of light was about three weeks, after which solid depletion and precipitation was observed. Photopolymerization of the gel **7** by irradiation at 254 nm with a 6 W UV lamp at a distance of 10 cm for 24 h led to a remarkable color change to intense blue (Figure 7A), accompanied by the appearance of an absorption band in the visible region with a maximum at 605 nm (Figure 7B). These results reflect the formation of poly(diacetylenes) as the result of 1,4-addition reaction of the diyne groups in the gel phase. Although it is well-known that the photopolymerization reaction is really efficient only in highly organized systems, the intense blue color observed after irradiation implies the extension of the π-delocalization along the polymerized nanotube.[90] The formation of conjugated poly(diacetylene) backbone of alternating enyne groups rigidifies the glyconanotube wall, resulting in a robust gel with temporal stability beyond one year. The structure of the polymerized hydrogel

dx.doi.org/10.1021/cm4022613 | *Chem. Mater.* 2013, 25, 4250–4261

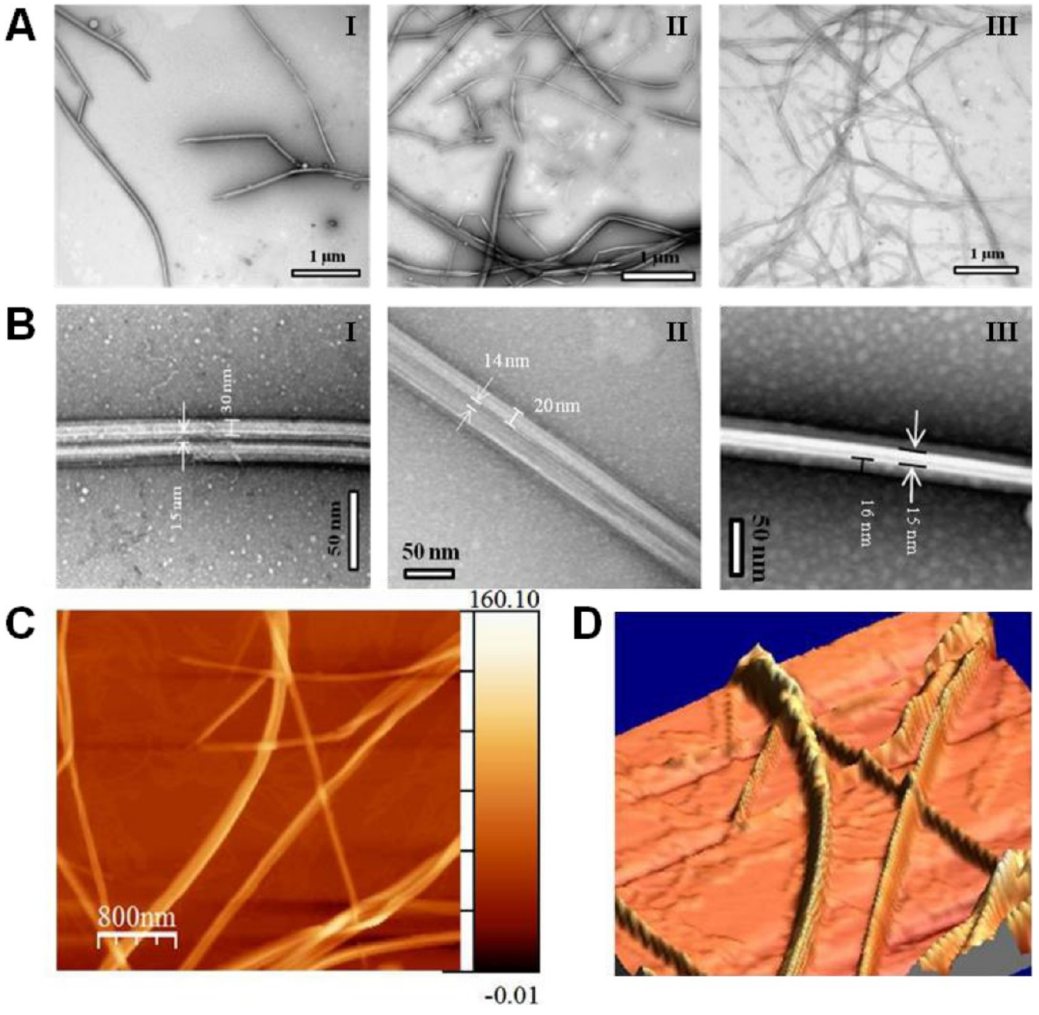

Figure 6. Large-scale height (A) and enlarged phase (B) TEM images of spherical nanotubes formed by self-organization of neoglycolipid **6** (I), **7** (II), and **8** (III). Bidimensional (C) and tridimensional (D) AFM images obtained by the tapping mode of a water-solution drop of helical nanotubes formed by self-organization of **8** in water, after deposition and drying on a just exfoliated mica plate.

formed from amphiphile **7** was further characterized by TEM, SEM, and AFM microscopies (Figure 7C–E). Meshes of agglomerated tubule with uniform diameters (50–70 nm) and lengths in the micrometer scale were consistently found in the photopolymerized hydrogel **7** under TEM (Figure 7C). However, in comparison with nonpolymerized gel no significant morphological differences were found for the polymerized xerogel **7**. This observation has been ascribed to the tube-like preorganization of glycolipid **7** molecules by intermolecular hydrogen-bonding and π-stacking forces of the amido and triazole groups respectively in nonpolymerized gel, in such a way that the subsequent photopolymerization reaction just fixed covalently the structure without altering the primary structure. The observation of the photopolymerized xerogel **7** under SEM at the hundreds of micrometer scale showed interesting intertwined and twisted structures similar to posies in a bush-form (Figure 7D). Moreover HR-SEM, allowed observing the intimate fibrillar aggregates composing the posies shown on the standard SEM images (Figure 7D). Going into an intermediate scale (1 μm), AFM microscopy showed a dense material composed by intercrossed and well-packed bundles of smaller and overlapped fibers, mimicking the seams in a cloth patch (Figure 7E). On the other hand, HR-AFM corroborated the aforementioned TEM data turning on fiber widths at around 52–67 nm (z-axis in the tapping mode).

Fourier transform infrared (FT-IR) measurements were performed to understand the nature of the interactions that participate in the assemblies (Figure 8). It is known that both amide I and amide II bands become weaker and shift into lower wavenumber when passing from free to H-bonded amide groups.[91] Something similar happens with the vibration of 1,2,3-triazole rings in π–π stacked aggregates. As such, the starting neoglycolipid **7** exhibits the amide I and II vibration modes at 1636 and 1550 cm^{-1}, respectively, while in the condensed phase the same peaks appeared at around ~1628 and ~1547 cm^{-1} values, together with a decreased intensity in both the dilute solutions and photopolymerized hydrogel (Figure 8A). In a similar way, the peak at 1480 cm^{-1} assigned to a stretching mode of the 1,2,3-triazole ring,[92] weaken and shifted at ~1475 cm^{-1} in both examples. On the other hand, the symmetric and antisymmetric CH_2 stretching bands of the alkyl chains are found without modification at ~2850 and ~2920 cm^{-1}, respectively, thus indicating a well packing and arrangement in *all-trans* conformation and light disorder in the different structures. These values highlight a cooperative self-assembly involving hydrogen bonding, π–π stacking and hydrophobic interactions simultaneously.

dx.doi.org/10.1021/cm4022613 | *Chem. Mater.* 2013, 25, 4250–4261

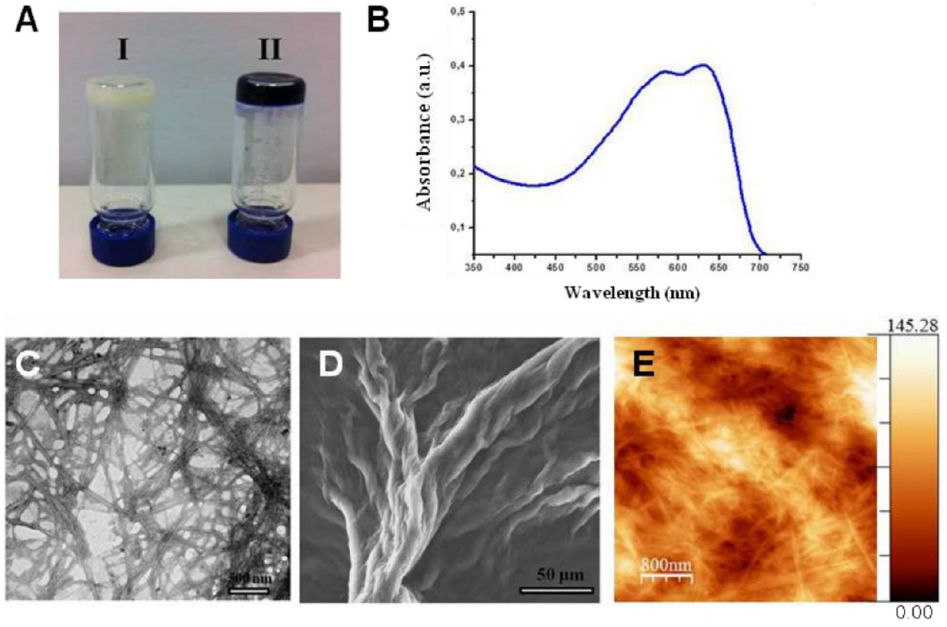

Figure 7. Photographs of vials showing the formation of hydrogel from neoglycolipid **7** and the chromatic change from white to blue upon irradiation at 254 nm with a 6 W UV lamp, highlighting the polymerization within the gel phase and the formation of PDA, accompanied by the appearance of an absorption band in the visible region with a maximum at 605 nm (B). TEM (C), SEM (D), and AFM (E) micrographs of xerogel derived from **7** on Cu grids (C and D) and on just-exfoliated mica (E).

Complementary small-angle X-ray scattering (SAXS) studies allowed stating the intimate structure of the hydrogel derived from **7**. Maximum peaks corresponding to averaged repeating distances of ca 9.8 nm was obtained (Figure 8B). Taking into account that the estimated size of a bilayer comprising two molecules of **7** with the alkyl-diyne chains in the center is 10 nm long (Figure 8D), the values match with a structure formed up by two concentric bilayers of glycolipids arranged in a tubular fashion in agreement with TEM results (~ 20 nm), as depicted in the sketch in Figure 8C. Based on these results, we suggest that the 1D-tubular supramolecular structures formed by the clicked glycolipids are stabilized by hydrogen bonds between the amide, the solvophobic interactions of the alkyl chains, and the $\pi-\pi$ interactions between the triazole rings (Figure S12 in the SI).

However, compound **1**, which self-organizes into micelles has all the aforementioned interactions with the exception of the claimed $\pi-\pi$ interactions. This observation raises the question if the driving force in the self-organization into 1D-nanomaterials is consequence of the structural restriction imposed by the $\pi-\pi$ interaction or if it is simply a result of the higher number of interactions involved in clicked nanotubes **2, 6–8** with regard to glycolipid **1**. In other words: What structure would result if we change the triazole ring by a different functional group able to establish further interaction such as hydrogen bonding for instance? At this point, it is worthy of mention that one reason at the basis of the great success of CuAAC in different research fields is the claim that the triazole ring act as a robust nonhydrolyzable amide mimic.[93] Structurally, the 1,4-disustituted 1,3 triazole can indeed mimic the *E* amide bond, with the N-3 electrons acting as the carbonyl oxygen of the amide, the polarization of the C5–H bond allows it to act as a hydrogen bond donor equivalent to the N–H bond of the amide, while the electrophilic and polarizable nature of the C-4 is electronically similar to the carbonyl carbon of the amide. Additionally, taking into account that the dipole moment of the triazole ring is higher than that of the amide bond, its hydrogen donor–acceptor properties are higher than those of the amide.

Based on these premises, we synthesized glycolipid **9**, similar to **7** with the exception that an amide function has been included instead of the triazole ring (Figure 9). The synthesis of the sought glycolipid was done starting from the amine **10** obtained in 80% yield from the common azide derivative used previously in the synthesis of **7** by catalytic hydrogenation. Condensation of the amine with *N*-Boc glycine **11** using DIPC as activator in the presence of DMAP afforded the Boc derivative **12** in 63% yield (Figure 9, step a). Boc-deprotection was accomplished by using trifluoroacetic acid in methylene chloride, leading to the free amine **13** in good yield (Figure 9, step b). Subsequently, condensation of the amine with 10,12-pentacosadiinoic acid (PCDA) **14** in the presence of TBTU and DMAP afforded the fully protected glycolipid **15** in 52% yield (Figure 9, step c). Finally, Zemplen deacetylation followed by purification of the product with G-20 sephadex column turned out pure glycolipid **9** (Figure 9, step d).

Once in hand, neoglycolipid **9** was submitted to the same conditions than those used for the formation of nanotubes and gel from **7** (Figure 9, step e). In this case, a clear solution was obtained with no apparent formation of nanotubes or gel neither at 0.1% nor at 1% concentration. The TEM analysis of the clear solution obtained, reveals the formation of spherical micelles with 8 nm diameter.

This result refutes the generalized assumption that the triazole ring is a good amide bond mimic and indicate that, at the supramolecular level, the claimed analogy should be used with extreme precaution as they can, and indeed do, generate completely different supramolecular assemblies. We ascribe this behavior to the ability of the triazole ring to establish effective $\pi-\pi$ interactions, and also to the larger distance between the triazole substituents, connected by three atoms, compared with

dx.doi.org/10.1021/cm4022613 | *Chem. Mater.* 2013, 25, 4250–4261

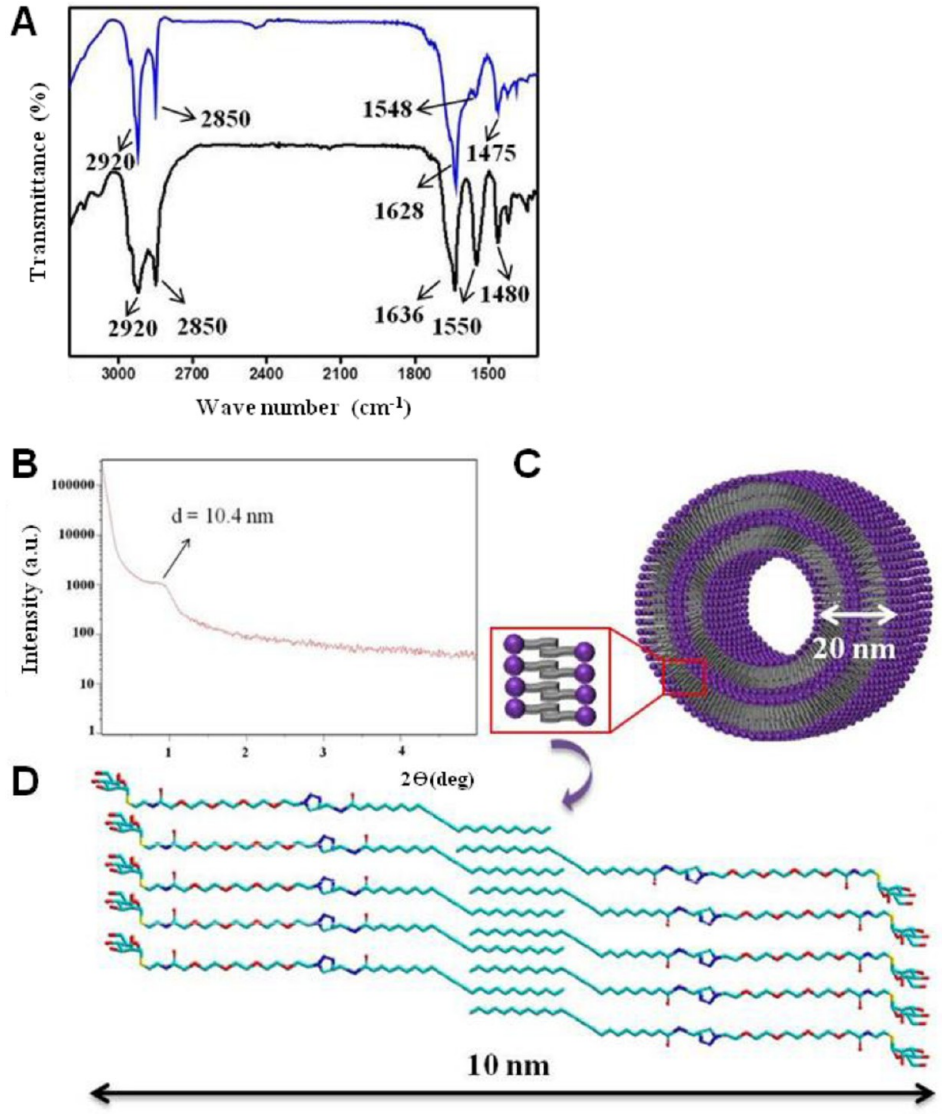

Figure 8. (A) FT-IR spectra of free neoglycolipid 7 (black) and self-assembled hydrogel (blue). (B) Small angle X-ray scattering of hydrogel derived from neoglycolpid 7. (C) Model of the molecular bilayer nanotube derived from SAXS study. (D) Hyperchem schematic illustration of the molecular packing in the self-assembled state.

those of the amide connected only with two atoms, with a global increase of 1.1 Å.

Study of Topotecan Release from Prepared PDA Hydrogels. It has been recently demonstrated that the controlled and constant supply of targeted anticarcinogenic drugs results in a better prognostic and cure of certain cancers than the administration of nonspecific medicines at tolerated maximum doses in reiterative cycles.[94] In this regard, a slow but constant and controlled release of anticarcinogen quantities has been achieved, for instance, by means of implants of antitumoral-swollen gels, resulting in an increased global efficacy.[95]

Despite the wide use of DMSO-based organogels for this and other pathologies,[96,97] hydrogels are the more desirable biocompatible materials for controlled release and for bioadhesive and targetable devices of therapeutic agents. This fact is ascribed to the specific control of drug release rate that can be achieved, while maintaining the pharmacologically effective drug levels for extended periods of time in blood, through oral, rectal, ocular, epidermal, or subcutaneous administration or even by the direct implantation into the body.[98] Within the tested gels, polymeric hydrogels exhibit a similar range of physical, chemical, and biological properties for biocompatible drug delivery systems than discrete molecules-based hydrogels, but offering the possibility to give controlled, pulsed, and triggered drug release profiles in a variety of tissues while maintaining their mechanical integrity.[99] Surprisingly, as far as we know, no preliminary studies on controlled release of drugs have been yet reported for robust PDA-based hydrogels.

With this aim in mind, we conducted some preliminary studies directed toward the utilization of polymerized PDA hydrogel 7 as a drug delivery depot system and stabilizer of the chemo-therapeutic drug topotecan (TPT) in order to determine its controlled-release properties (Figure 10).[100,101] TPT is a hemisynthetic analogue of the alkaloid camptothecin, a natural cytotoxic compound with high anticarcinogenic activity against breast, colon, ovary, and lung tumors. In contrast to camptothecin, TPT is soluble in water thanks to the tertiary amine at C-9 position, but similar to other CPT-family drugs, suffer from poor stability and from the preponderance of

dx.doi.org/10.1021/cm4022613 | Chem. Mater. 2013, 25, 4250−4261

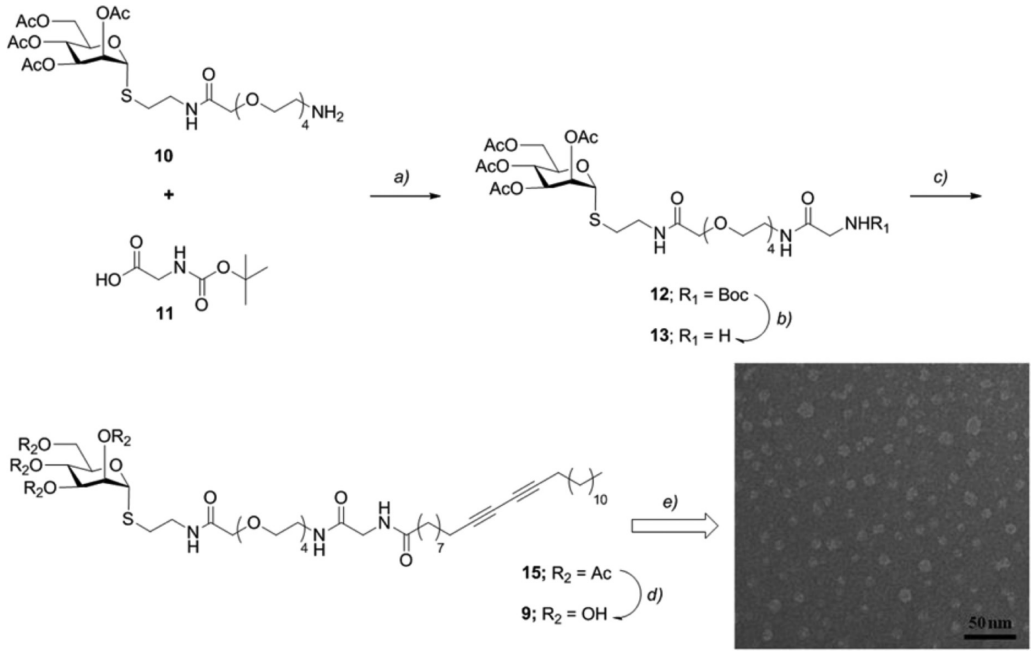

Figure 9. Synthesis of neoglycolipid **9**: (a) DIPC, DMAP, CH_2Cl_2, rt, 16 h; (63%), (b) TFA, CH_2Cl_2, rt, 5 h; (99%.), (c) (i) PCDA (**14**), TBTU, DIPEA, DMF, rt, 5 min. (ii) **13**, DIPEA, DMF, rt, 14 h; (52%), (d) (i) NaOMe, MeOH, rt; 1 h. (ii) Amberlyst Ir-120; (82%), (e) H_2O, 50 °C; together with a TEM image showing the resulting self-organization in water in a micellar fashion.

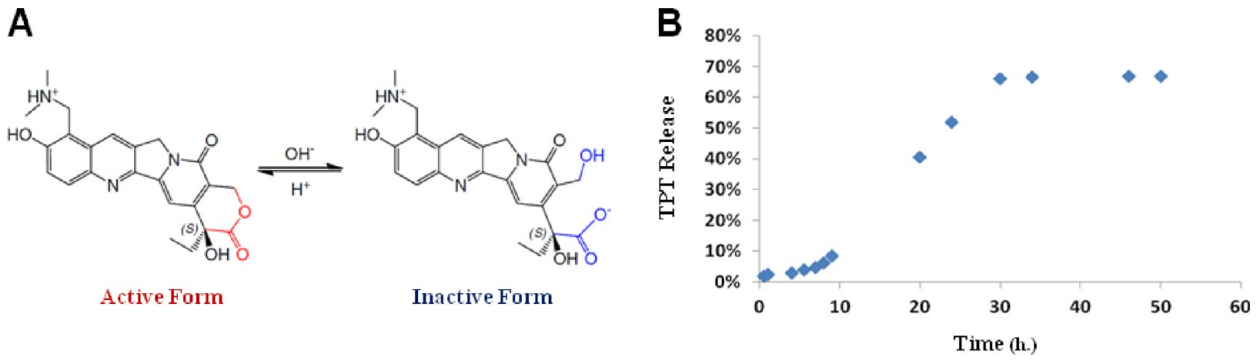

Figure 10. (A) Hydrolysis reaction of TPT from the active lactone form (red) to the inactive carboxylate form (blue) at physiologic pH. (B) Preliminary study by absorption spectrophotometry of the TPT release in water from TPT-containing hydrogel **7** vs time.

a less active carboxylate form over the active lactone form at physiologic pH (Figure 10A).

The synthesis of TPT/gel complex was carried out by dissolving 100 μg of TPT in an aqueous solution of **7** (1 mg/100 μL) followed by gel formation, as described before. Upon irradiation at 254 nm for 24 h, the color of the gel-TPT assembly changed from white to deep blue, indicating that the polymerization takes place ensuring the complete entrapping of the chemo-medicine within the polymeric framework in the form of the composite TPT/gel-**7**.

Freshly prepared hydrogel TPT/gel-**7** was disposed in a test vial containing Milli-Q water (1.00 mL) at 37.0 °C. Afterward, aliquots of identical volume of the supernatant were taken at different intervals of time, filling up to 1.00 mL and the absorptions at 381 nm recorded in a spectrophotometer. The absorbance data were corrected and converted into concentration values according to the previously stated Lambert−Beer law and the calculated molar extinction coefficient from standards of TPT at 37 °C (for more details, see SI). As deduced from sigmoid curve of Figure 10 and the reach of a plateau, a maximum percentage value of TPT release at around 67% from hydrogel TPT/**7** was attained at t = 30 h (Figure 10B). In comparison with the few examples in the literature including cross-linked TPT-containing hydrogels, we obtained a minor release percentage than that of a poly(ethyleneglycol) copolymer with vinylsulphone cross-linker.[100] To the contrary, the TPT/gel-**7** system resulted in a 3-fold more prolonged release time than the cited example.

■ CONCLUSIONS

In conclusion, we have synthesized a series of glycolipids by means of convergent synthetic pathways that include as key ligation reaction either CuAAC or amidation, resulting in amphiphiles with 1,2,3-trizolo or amido groups, respectively. From the comparison of the supramolecular self-organization in water, we have observed that the neoglycolipids with an amide ligating the hydrophilic and hydrophobic part of the amphiphile afford tridimensional micelles, while those having a triazole self-organize into 1D-nanotubes. Additionally, at higher concentration (1%), the clicked amphiphiles form hydrogels through three-dimensional networks of bundled nanotubes. Photo-

dx.doi.org/10.1021/cm4022613 | *Chem. Mater.* 2013, 25, 4250−4261

polymerization of obtained nanomaterials by irradiation at 254 nm leads to the formation of conjugated poly(diacetylene) backbones of alternating enyne groups, which rigidify the glyconanomaterials, thus enhancing their physical stability, a critical issue for their future medical uses. The 1D-based nanomaterials have an intense blue color, indicative of the long-range π-delocalization along the polymerized nanotube, and are excellent sensors of the surrounding media able to change their color to red as a consequence of heat (thermochromism) or solvent (solvatochromism). The obtained nanostructures were extensively characterized using TEM and AFM techniques, enabling the confirmation of the formation of tubular structures in water for all triazolo-substituted neoglycolipids (**2**, **6**−**8**) and micellar structures for the glycolipid containing an amide group (**1** and **9**). This fact refutes the so-called isosteric character of 1,2,3-triazole and amide groups, at least at the supramolecular level, and points to the possibility of using the CuAAC between azides and alkynes to create supramolecular diversity at the nanoscale. According to SAXS, FT-IR, and molecular modeling, the resulting structures are explained in terms of glycolipidic bilayers associated in concentric tubules, with all the association motifs participating in the assembly. The functionality of the latter has been, moreover, evaluated as a drug releaser of topotecan, giving rise to a maximum release value of ca. 67% after 30 h.

A salient feature of our designed functional monomers is the formation of biologically active hydro-soluble nanomaterials exposing a dense layer of carbohydrates to the water phase similar to the glycocalyx at the cell surface. In this sense, recent investigations have confirmed the prime importance of carbohydrates in important biological events including cell−cell communication, cell adhesion, fertilization, differentiation, development, inflammation, tumor cell metastasis, and pathogen infections.[102,103] Therefore, the polymerized nanomicelles, which are covered by a dense carbohydrate array can be used as synthetic multivalent systems to treat pathologies mediated by carbohydrate−lectin interactions. Additionally, the presence of a poly(ethyleneglycol) (PEG) fragment—known to reduce the rapid uptake and clearance in vivo by the cell mononuclear phagocytic system—makes the formed nanomicelles excellent nanovectors for the active targeting of hydrophobic antitumoral molecules. On the other hand, the formed hydrogels mimic the extracellular matrix and, as such, are excellent materials for tissue engineering. Moreover, the nanotube-based 3D-nanogels can also encapsulate biologically active molecules including proteins in the inner hollow cavity of the tubules, preventing their fast denaturation behavior and therefore, keeping their biological activity. Based on our findings and on the previously reported works, the applications of both polymerized micelles and LNT-based hydrogels as smart nanocontainers for active drug delivery and as 3D-matrix for tissue engineering are being actively investigated in our laboratories, and the results will be reported in due courses.

EXPERIMENTAL SECTION

General Procedure for the Preparation of Self-Assembled Hydrogels. The preparation of the hydrogels was performed by dissolving 1 mg of neoglycolipid **2**, **6**−**8** in 100 μL of water and heating the suspension to 50 °C during 30 min. Then, the clear solutions were cooled to room temperature, thus inducing the gelification of the mixture. Irradiation at 254 nm with a 6W UV lamp at a distance of 10 cm of the vial for 24 h led to the photopolymerization of the diacetylenic tails into self-assembled nanotubes, as demonstrated by the remarkable color change from white to intense blue.

Preparation of Gel-7/TPT Inclusion Complex. TPT (100 μg) was dissolved in an aqueous solution of neoglycolipid **7** (1 mg/100 μL). After heating to 50 °C during 30 min, the solution was allowed to cool to room temperature inducing the formation of the hydrogel-**7**/TPT inclusion complex. Next, the photopolymerization of the diacetylenic tails as described before afforded the polymerized blue-colored hydrogel-**7**/TPT complex with high stability.

ASSOCIATED CONTENT

Supporting Information

Detailed methods and additional figures. This material is available free of charge via the Internet at http://pubs.acs.org.

AUTHOR INFORMATION

Corresponding Author

*Tel: +34 95 448 9559. Fax: +34 954460565. E-mail: khiar@iiq.csic.es.

Notes

The authors declare no competing financial interest.

ACKNOWLEDGMENTS

This work was supported by the Ministerio de Economía y Competitividad (Grant No. CTQ2010-21755-CO2-01) and the Junta de Andalucía (Grant Nos. P07-FQM-2774 and P08-CTS-04297). We acknowledge CITIUS for TEM, AFM, and NMR facilities. Dr. M. Assali thanks the MAEC-AECID for PhD scholarship. Dr. J.-J. Cid thanks CSIC for the postdoctoral JAE DOC scholarship.

REFERENCES

(1) Zhang, S. G. *Nat. Biotechnol.* **2003**, *21*, 1171−1178.
(2) Cranford, S. W.; de Boer, J.; van Blitterswijk, C.; Buehler, M. J. *Adv. Mater.* **2013**, *25*, 802−824.
(3) Kim, S.; Park, C. B. *Adv. Funct. Mater.* **2013**, *23*, 10−25.
(4) Aida, T.; Meijer, E. W.; Stupp, S. I. *Science* **2012**, *335*, 813−818.
(5) Rybtchinski, B. *ACS Nano* **2011**, *5*, 6791−6818.
(6) Dvir, T.; Timko, B. P.; Kohane, D. S.; Langer, R. *Nat. Nanotechnol.* **2011**, *6*, 13−22.
(7) Whitesides, G. M.; Mathias, J. P.; Seto, C. T. *Science* **1991**, *254*, 1312−1319.
(8) Lehn, J. M. *Proc. Natl. Acad. Sci. U.S.A.* **2002**, *99*, 4763−4768.
(9) Lehn, J. M. *Science* **2002**, *295*, 2400−2403.
(10) Whitesides, G. M. *Small* **2005**, *1*, 172−179.
(11) Lim, Y.-b.; Moon, K.-S.; Lee, M. *Chem. Soc. Rev.* **2009**, *38*, 925−934.
(12) Otsuka, H. *Adv. Drug Delivery Rev.* **2003**, *55*, 403−419.
(13) Pack, D. W.; Hoffman, A. S.; Pun, S.; Stayton, P. S. *Nat. Rev. Drug Discovery* **2005**, *4*, 581−593.
(14) He, Y.; Ye, T.; Su, M.; Zhang, C.; Ribbe, A. E.; Jiang, W.; Mao, C. *Nature* **2008**, *452*, 198−201.
(15) Mammen, M.; Choi, S. K.; Whitesides, G. M. *Angew. Chem., Int. Ed.* **1998**, *37*, 2755−2794.
(16) Kiessling, L. L.; Gestwicki, J. E.; Strong, L. E. *Angew. Chem., Int. Ed.* **2006**, *45*, 2348−2368.
(17) Barnard, A.; Smith, D. K. *Angew. Chem., Int. Ed.* **2012**, *51*, 6572−6581.
(18) Badjic, J. D.; Nelson, A.; Cantrill, S. J.; Turnbull, W. B.; Stoddart, J. F. *Acc. Chem. Res.* **2005**, *38*, 723−732.
(19) Levine, P. M.; Carberry, T. P.; Holubb, J. M.; Kirshenbaum, K. *Med. Chem. Commun.* **2013**, *4*, 493−509.
(20) Petkau-Milroy, K.; Brunsveld, L. *Org. Biomol. Chem.* **2013**, *9*, 219−232.
(21) Lee, M.; Cho, B.-K; Zin, W.-C. *Chem. Rev.* **2001**, *101*, 3869−3892.

(22) Percec, V.; Dulcey, A. E.; Balagurusamy, V. S. K.; Miura, Y.; Smidrkal, J.; Peterca, M.; Nummelin, S.; Edlund, U.; Hudson, S. D.; Heiney, P. A.; Dunan, H.; Magonov, S. N.; Vinogradov, S. A. *Nature* **2004**, *430*, 764−768.
(23) Elemans, J. A. A. W.; Rowan, A. E.; Nolte, R. J. M. *J. Mater. Chem.* **2003**, *13*, 2661−2670.
(24) Alam, M. A.; Kim, Y.-S.; Ogawa, S.; Tsuda, A.; Ishii, N.; Aida, T. *Angew. Chem., Int. Ed.* **2008**, *47*, 2070−2073.
(25) Mailänder, V.; Landfester, K. *Biomacromolecules* **2009**, *10*, 2379−2400.
(26) Albanese, A.; Tang, P. S.; Chan, W. C. W. *Ann. Rev. Biomed. Eng.* **2012**, *14*, 1−16.
(27) Massignani, M.; LoPresti, C.; Blanazs, A.; Madsen, J.; Armes, S. P.; Lewis, A. L.; Gattaglia, G. *Small* **2009**, *5*, 2424−2432.
(28) Ryu, J.-H.; Lee, E.; Lim, Y.-b.; Lee, M. *J. Am. Chem. Soc.* **2007**, *129*, 4808−4814.
(29) Lim, Y.-b.; Park, S.; Lee, E.; Ryu, J.-H.; Yoon, Y.-R.; Kim, T.-H.; Lee, M. *Chem. Asian. J.* **2007**, *2*, 1363−1369.
(30) *Organic Nanostructures*; Atwood, J. L.; Steed, J. W., Eds.; Wiley-VCH: Weinheim, Germany, 2008.
(31) Sangeetha, N. M.; Maitra, U. *Chem. Soc. Rev.* **2005**, *34*, 821−836.
(32) Steed, J. W. *Chem. Commun* **2011**, *47*, 1379−1383.
(33) Truong, W. T.; Su, Y.; Meijer, J. T.; Thordarson, P.; Braet, F. *Chem. Asian. J.* **2011**, *6*, 30−42.
(34) Hoffman, A. S. *Adv. Drug Delivery Rev.* **2012**, *64*, 18−23.
(35) Seliktar, D. *Science* **2012**, *336*, 1124−1128.
(36) Ellis-Behnke, R. G; Liang, Y.-X.; You, S.-W.; Tay, D. K. C.; Zhang, S.; So, K.-F.; Schneider, G. E. *Proc. Natl. Acad. Sci. U.S.A.* **2006**, *103*, 5054−5059.
(37) Silva, G. A.; Czeisler, C.; Niece, K. L.; Beniash, E.; Harrington, D. A.; Kessler, J. A.; Stupp, S. I. *Science* **2004**, *303*, 1352−1355.
(38) Yang, Z.; Liang, G.; Ma, M.; Abbah, A. S.; Lu, W. W.; Xu, B. *Chem. Commun.* **2007**, 843−845.
(39) van Brommel, K. J. C.; Friggeri, A.; Shinkai, S. *Angew. Chem., Int. Ed.* **2003**, *42*, 980−999.
(40) Sada, K.; Takeuchi, M.; Fujita, N.; Numata, M.; Shinkai, S. *Chem. Soc. Rev.* **2007**, *36*, 415−436.
(41) Fukushima, T.; Asaka, K.; Kosaka, A.; Aida, T. *Angew. Chem., Int. Ed.* **2005**, *44*, 2410−2413.
(42) Puigmartí-Luis, J.; Laukhin, V.; Pérez del Pino, Á.; Vidal-Gancedo, J.; Rovira, C.; Laukhina, E.; Amabilino, D. B. *Angew. Chem., Int. Ed.* **2007**, *46*, 238−241.
(43) Haines-Butterick, L.; Rajagopal, K.; Branco, M.; Salick, D.; Rughani, R.; Plarz, M.; Lamm, M. S.; Pochan, D. J.; Schneider, J. P. *Proc. Natl. Acad. Sci. U.S.A.* **2007**, *104*, 7791−7796.
(44) Li, X.; Li, J. *J. Biomed. Mater. Res.* **2007**, *86A*, 1055−1061.
(45) Vemula, P. K.; Cruikshank, G. A.; Karp, J. M.; John, G. *Biomaterials* **2009**, *30*, 383−393.
(46) Wang, H.; Yang, Z. *Soft Matter* **2012**, *8*, 2344−2347.
(47) Hirst, A. R.; Coates, I. A.; Boucheteau, T. R.; Miravet, J. F.; Escuder, B.; Castelletto, V.; Hamley, I. W.; Smith, D. K. *J. Am. Chem. Soc.* **2008**, *130*, 9113−9121.
(48) Gravel, E.; Ogier, J.; Arnauld, T.; Mackiewicz, N.; Ducongé, F.; Doris, E. *Chem.—Eur. J.* **2012**, *18*, 400−408.
(49) Kang, S. H.; Jung, B. M.; Kim, W. J.; Chang, J. Y. *Chem. Mater.* **2008**, *20*, 5532−5540.
(50) Wegner, G. Z. *Naturforsch, B: Anorg. Chem. Org. Chem. Biochem. Biophys. Biol.* **1969**, *24*, 824−827.
(51) Day, D.; Ringsdorf, H. *J. Polym. Sci., Polym. Lett. Ed.* **1978**, *16*, 205−210.
(52) Reppy, M. A.; Pindzola, B. A. *Chem. Commun.* **2007**, 4317−4388.
(53) Lauher, J. W.; Fowler, F. W.; Goroff, N. S. *Acc. Chem. Res.* **2008**, *41*, 1215−1229.
(54) Yoon, B.; Lee, S.; Kim, J.-M. *Chem. Soc. Rev.* **2009**, *38*, 1958−1968.
(55) Sun, X.; Chen, T.; Huang, S.; Li, L.; Peng, H. *Chem. Soc. Rev.* **2010**, *39*, 4244−4257.
(56) Yarimaga, O.; Jaworski, J.; Yoon, B.; Kim, J.-M. *Chem. Commun.* **2012**, *48*, 2469−2485.
(57) Singh, A.; Thompson, R. B.; Schnur, J. M. *J. Am. Chem. Soc.* **1986**, *108*, 2785−2787.
(58) Yuan, Z.; Lee, C.-W.; Lee, S.-H. *Angew. Chem., Int. Ed.* **2004**, *43*, 419.
(59) Ahn, D. J.; Lee, S.; Kim, J.-M. *Adv. Funct. Mater.* **2009**, *19*, 1483−1496.
(60) Chance, R. R. *Macromolecules* **1980**, *13*, 396−398.
(61) Bloor, D. *Macromol. Chem. Phys.* **2001**, *202*, 1410−1423.
(62) Nallicheri, R. A.; Rubner, M. F. *Macromolecules* **1991**, *24*, 517−525.
(63) Carpick, R. W.; Sasaki, D. Y.; Burns, A. R. *Langmuir* **2000**, *16*, 1270−1278.
(64) Chen, X.; Li, L.; Sun, X.; Liu, Y.; Luo, B.; Wang, C.; Bao, Y.; Xu, H.; Peng, H. *Angew. Chem., Int. Ed.* **2011**, *50*, 5486−5489.
(65) Charych, D. H.; Nagy, J. O.; Spevak, W.; Bednarski, M. D. *Science* **1993**, *261*, 585−588.
(66) Wu, J.; Zawistowski, A.; Ehrmann, M.; Yi, T.; Schmuck, C. *J. Am. Chem. Soc.* **2011**, *133*, 9720−9723.
(67) Chen, X.; Kang, S.; Kim, M. J.; Kim, J.; Kim, Y. S.; Kim, H.; Chi, B.; Kim, S.-J.; Lee, J. Y.; Yoon, J. *Angew. Chem., Int. Ed.* **2010**, *49*, 1422−1425.
(68) Kim, K. M.; Oh, D. J.; Ahn, K. H. *Chem.−Asian J.* **2011**, *6*, 122−127.
(69) Pevzner, A.; Kolusheva, S.; Orynbayeva, Z.; Zelinek, R. *Adv. Funct. Mater.* **2008**, *18*, 242−247.
(70) Leal, M. P.; Assali, M.; Fernández, I.; Khiar, N. *Chem.−Eur. J.* **2011**, *17*, 1828−1836.
(71) Contal, E.; Klymchenko, A. S.; Mély, Y.; Meunier, S.; Wagner, A. *Soft Matter* **2011**, *7*, 1648−1650.
(72) Jiang, H.; Pan, X.-J.; Lei, Z.-Y.; Zou, G.; Zhang, Q.-J.; Wang, K.-Y. *J. Mater. Chem.* **2011**, *21*, 4518−4522.
(73) Zhou, W.; Li, Y.; Zhu, D. *Chem. Asian J.* **2007**, *2*, 222−229.
(74) Kameta, N.; Yoshida, K.; Masuda, M.; Shimizu, T. *Chem. Mater.* **2009**, *21*, 5892−5898.
(75) George, M.; Weiss, R. G. *Chem. Mater.* **2003**, *15*, 2879−2888.
(76) Shirakawa, M.; Shinkai, S. *J. Am. Chem. Soc.* **2005**, *127*, 4164−4165.
(77) Aoki, K.; Kudo, M.; Tamaoki, N. *Org. Lett.* **2004**, *6*, 4009−4012.
(78) Nagasawa, J.; Kudo, M.; Hayashi, S.; Tamaoki, N. *Langmuir* **2004**, *20*, 7907−7916.
(79) Khiar, N.; Pernía-Leal, M.; Baati, R.; Ruhlmann, C.; Mioskowski, C.; Schultz, P.; Fernández, I. *Chem. Commun.* **2009**, 4121−4123.
(80) Assali, M.; Pernía-Leal, M.; Fernández, I.; Khiar, N. *Nanotechnology* **2013**, *24*, 085201.
(81) Richard, C.; Balavoine, F.; Schultz, P.; Ebbesen, T. W.; Mioskowski, C. *Science* **2003**, *300*, 775−778.
(82) Islam, M. F.; Rojas, E.; Bergey, D. M.; Johnson, A. T.; Yodh, A. G. *Nano Lett.* **2003**, *3*, 269−273.
(83) Ke, P. U. *Phys. Chem.* **2007**, *9*, 439−447.
(84) Thauvin, C.; Rickling, S.; Schultz, P.; Célia, H.; Meunier, S.; Mioskowski, C. *Nat. Nanotechnol.* **2008**, *3*, 743−748.
(85) Assali, M.; Cid, J.-J.; Pernía-Leal, M.; Muñoz-Bravo, M.; Fernández, I.; Khiar, N. *ACS Nano* **2013**, *7*, 2145−2153.
(86) Kolb, H. C.; Finn, M. G.; Sharpless, K. B. *Angew. Chem., Int. Ed.* **2001**, *40*, 2004−2021.
(87) Rostovtsev, V. V.; Green, L. G.; Fokin, V. V.; Sharpless, K. B. *Angew. Chem., Int. Ed.* **2002**, *41*, 2596−2599.
(88) Tornoe, C. W.; Christensen, C.; Meldal, M. *J. Org. Chem.* **2002**, *67*, 3057−3064.
(89) Menger, F. M.; Karan, K. L. *J. Am. Chem. Soc.* **2000**, *122*, 11679−11691.
(90) Dautel, O. J.; Robitzer, M.; Lère-Porte, J.-P.; Serein-Spirau, F.; Moreau, J. J. E. *J. Am. Chem. Soc.* **2006**, *128*, 16213−16223.
(91) Bouas-Laurent, H.; Desvergne, J.-P. Optical Spectroscopic Methods as Tools to Investigate Gel Structures. In *Molecular Gels*; Weiss, R. G.; Terech, P., Eds.; Springer: Netherlands: 2006, pp 363.

(92) Katritzky, A. R.; Ramsden, C. A.; Joule, J. A. *Handbook of Heterocyclic Chemistry*; Elsevier: Oxford, 2010.
(93) Tron, G. C.; Pirali, T.; Billington, R. A.; Canonico, P. L.; Sorba, G.; Genazzani, A. A. *Med. Res. Rev.* **2008**, *28*, 278−308.
(94) Hochster, H.; Liebes, L.; Speyer, J.; Sorich, J.; Taubes, B.; Oratz, R.; Wernz, J.; Chachoua, A.; Raphael, B.; Vinci, R. Z. *J. Clin. Oncol.* **1994**, *12*, 553−559.
(95) Wang, C.; Varshney, R. R.; Wang, D.-A. *Adv. Drug Delivery Rev.* **2010**, *62*, 699−710.
(96) Swanson, B. N. *Rev. Clin. Basic Pharm.* **1985**, *5*, 1−33.
(97) Jacob, S. W. *Cryobiology* **1986**, *23*, 14−27.
(98) Nagai, T.; Machida, Y. *Adv. Drug Delivery Rev.* **1993**, *11*, 179−191.
(99) Bae, Y. H.; Kim, S. W. *Adv. Drug Delivery Rev.* **1993**, *11*, 109−135.
(100) Lalloo, A.; Chao, P.; Hu, P.; Stein, S.; Sinko, P. *J. Controlled Release* **2006**, *112*, 333−342.
(101) Chang, G.; Ci, T.; Yu, L.; Ding, J. *J. Controlled Release* **2011**, *156*, 21−27.
(102) Lis, H.; Sharon, N. *Chem. Rev.* **1998**, *98*, 637−674.
(103) Simanek, E. E.; McGarvey, G. J.; Jablonski, J. A.; Wong, C. H. *Chem. Rev.* **1998**, *98*, 833−862.